

Crystal Structure and Magnetic Properties of Two Isomeric Three-Dimensional Pyromellitate-Containing Cobalt(II) Complexes

Oscar Fabelo,[†] Jorge Pasán,[†] Laura Cañadillas-Delgado,[†] Fernando S. Delgado,[‡] Francesc Lloret,[§] Miguel Julve,[§] and Catalina Ruiz-Pérez^{*,†}

Laboratorio de Rayos X y Materiales Moleculares, Departamento de Física Fundamental II, Facultad de Física, Universidad de La Laguna, Avenida Astrofísico Francisco Sánchez s/n, E-38024 La Laguna, Tenerife, Spain, BM16-LLS European Synchrotron Radiation Facility, 6 Rue Jules Horowitz-BP 220, 38043 Grenoble Cedex 9, France, and Instituto de Ciencia Molecular (ICMol)/Departament de Química Inorgànica, Universitat de València, Polígono La Coma s/n, 46980 Paterna (València), Spain

Received April 22, 2008

The hydrothermal preparation, crystal structure determination, and magnetic study of two isomers made up of 1,2,4,5-benzenetetracarboxylate and high-spin Co^{II} ions of formula [Co₂(bta)(H₂O)₄]_n · 2nH₂O (**1** and **2**; H₄bta = 1,2,4,5-benzenetetracarboxylic acid) are reported. **1** and **2** are three-dimensional compounds whose structures can be described as (4,4) rectangular layers of *trans*-diaquacobalt(II) units with the bta⁴⁻ anion acting as tetrakis-monodentate ligand through the four carboxylate groups, which are further connected through other *trans*-[Co(H₂O)₂]²⁺ (**1**) and planar [Co(H₂O)₄]²⁺ (**2**) entities, with the bridging units being a carboxylate group in either the *anti*–*syn* (**1**) or *syn*–*syn* (**2**) conformations and a water molecule (**2**). The study of the magnetic properties of **1** and **2** in the temperature range 1.9–300 K shows the occurrence of weak antiferromagnetic interactions between the high-spin Co^{II} ions, with the strong decrease of $\chi_M T$ upon cooling being mainly due to the depopulation of the higher energy Kramers doublets of the six-coordinated Co^{II} ions. The computed values of the exchange coupling between the Co^{II} ions across *anti*–*syn* carboxylate (**1**) and *syn*–*syn* carboxylate/water (**2**) bridges are $J = -0.060$ (**1**) and -1.90 (**2**) cm⁻¹ (with the Hamiltonian being defined as $\hat{H} = -J\sum_{i,j}\hat{S}_i \cdot \hat{S}_j$). These values follow the different conformations of the carboxylate bridge in **1** (*anti*–*syn*) and **2** (*syn*–*syn*) with the occurrence of a double bridge in **2** (water/carboxylate).

Introduction

Research efforts on crystal engineering have grown exponentially because of the need of controlling the molecular organization in the solid state, with the main goal being the design and preparation of multifunctional materials with novel structures and promising properties.¹ However, the materialization of a desired metal–organic framework (MOF) in a truly deliberate manner appears as a quite

difficult task in most of the cases because of the influence of many factors upon the final product structures, such as the coordination geometry of the central metal ion and the shape, functionality, flexibility, and symmetry of the ligand. Polynuclear complexes with transition-metal ions and polycarboxylate ligands have received considerable attention because of their interesting structures and potential applications.² Aromatic tetracarboxylic derivatives such as 1,2,4,5-benzenetetracarboxylic acid (H₄bta, commonly known as pyromellitic acid) and their deprotonated forms (H_nbta⁽⁴⁻ⁿ⁾⁻) belong to the important family of polycarboxylate O-donor ligands, which have been extensively used to prepare

* To whom correspondence should be addressed. E-mail: caruiz@ull.es.
[†] Universidad de La Laguna.

[‡] BM16-LLS European Synchrotron Radiation Facility.

[§] Universitat de València.

- (1) (a) Kiang, Y. H.; Gardner, G. B.; Lee, S.; Xu, Z. T.; Lobkovsky, E. B. *J. Am. Chem. Soc.* **1999**, *121*, 8204. (b) Braga, D.; Desiraju, G. R.; Miller, J. S.; Orpen, A. G.; Price, S. L. *CrystEngComm* **2002**, *4*, 500. (c) Zhang, J.; Li, Z. J.; Kang, Y.; Cheng, J. K.; Yao, Y. G. *Inorg. Chem.* **2004**, *43*, 8085. (d) Lin, P.; Henderson, R. A.; Harrington, R. W.; Clegg, W.; Wu, C. D.; Wu, X. T. *Inorg. Chem.* **2004**, *43*, 181.

- (2) (a) Yaghi, O. M.; Li, H.; Davis, C.; Richardson, D.; Groy, T. L. *Acc. Chem. Res.* **1998**, *31*, 474. (b) Choi, H. J.; Lee, T. S.; Suh, M. P. *Angew. Chem., Int. Ed.* **1999**, *38*, 1405. (c) Eddaoudi, M.; Moler, D. B.; Li, H.; Chen, B.; Reineke, T. M.; O'Keeffe, M.; Yaghi, O. M. *Acc. Chem. Res.* **2001**, *34*, 319.

MOFs.^{3–6} The variations in the possible binding modes of its four potentially coordinating carboxylic/carboxylate groups along with the different coordination preferences of the metal ions can give rise to a great variety of interesting structures. They can be classified into two series: the first one is built up from isolated metal aggregates that are made up of single-metal-centered polyhedra (tetrahedron, square pyramid, octahedron, etc.) or an arrangement of several polyhedral units;⁷ the second one shows infinite polymeric arrangements, usually composed of MO₆ octahedra linked each other through the carboxylate ligands.⁸

The versatility as ligands of the partially or totally deprotonated forms of H₄bta toward the Co^{II} ions together with the structural effects caused by their behavior as intra- and intermolecular hydrogen-bond donors and/or acceptors has been illustrated by previous works.⁹ Within the aim to get deeper insights on the coordination chemistry of pyromellitate-containing cobalt(II) complexes, we have prepared two new three-dimensional compounds of formula [Co₂(bta)(H₂O)₄]_n·2nH₂O (**1** and **2**). Their synthesis, single-crystal X-ray characterization, and magnetic characterization are reported in this contribution.

Experimental Section

Materials and Methods. Reagents and solvents used in the syntheses of **1** and **2** were purchased from commercial sources and used without further purification. The preparative hydrothermal method that allowed us to grow X-ray-quality crystals of these compounds is described herein. Elemental analyses (C and H) were performed with an EA 1108 CHNS/O automatic analyzer.

Synthesis of the Complexes. Co₂(bta)(H₂O)₄]_n·2nH₂O (**1**). The pH of an aqueous solution (20 mL) of H₄bta (0.12 g, 0.5 mmol) was adjusted to 5.0 by the dropwise addition of another aqueous solution of 0.1 M NaOH. Cobalt(II) chloride hexahydrate (0.119 g, 0.5 mmol) dissolved in a minimum amount of water was added to the aforementioned solution under continuous stirring. The

resulting reddish mixture was sealed in a 45 mL stainless steel reactor with a Teflon liner and heated at 115 °C for 48 h. After cooling, X-ray-quality crystals of **1** as pink prisms were removed from the remaining mother liquor, washed with ethanol, and air-dried. Anal. Calcd for C₁₀H₁₄Co₂O₁₄ (**1**): C, 25.23; H, 2.96. Found: C, 25.19; H, 2.88.

[Co₂(bta)(H₂O)₄]_n·2nH₂O (**2**). An aqueous solution (5 mL) of Na₂CO₃ (0.1 g, 1 mmol) was poured into another aqueous solution (20 mL) of H₄bta (0.12 g, 0.5 mmol) under continuous stirring at room temperature. Cobalt(II) chloride hexahydrate (0.238 g, 1 mmol) dissolved in a minimum amount of water was added to the above-mentioned solution. The resulting mixture was sealed in a 45 mL stainless steel reactor with a Teflon liner and heated at 90 °C for 98 h. After cooling, X-ray-quality crystals of **2** as violet prisms were removed from the solution. They were washed with ethanol and air-dried. Anal. Calcd for C₁₀H₁₄Co₂O₁₄ (**2**): C, 25.23; H, 2.96. Found: C, 25.38; H, 2.72.

Crystal Structure Determination and Refinement. Single-crystal X-ray diffraction data sets were collected at 293 K (**1**) and at 100 K (**2**) on a Nonius Kappa CCD diffractometer with graphite-monochromated Mo K α radiation (0.710 73 Å). The data were indexed, integrated, and scaled using the EVALCCD program.¹⁰ Crystal parameters and refinement results for **1** and **2** are summarized in Table 1. The structures of **1** and **2** were solved by direct methods using the SHELXS97 computational program.¹¹ All non-H atoms were refined anisotropically through a full-matrix least-squares technique based on F² with SHELX97. The crystallization water molecules O3w and O4w in **1** were refined with an occupancy factor of 0.5 because of the short distance [1.934(9) Å] between the two peaks in the Fourier map corresponding to the solvent molecules. The hydrogen atoms of **1** and **2** (except those of the water molecules in **2**) were geometrically positioned and included in the least-squares calculations with a riding model. The hydrogen atoms of the water molecules in **2** were located from difference Fourier maps and refined with isotropic temperature factors. The final geometrical calculations and the graphical manipulations were

- (3) (a) Dalai, S.; Mukherjee, P. S.; Zangrando, E.; Lloret, F.; Chaudhuri, N. R. *J. Chem. Soc., Dalton Trans.* **2002**, 822. (b) Zhang, L.-J.; Xu, J.-Q.; Shi, Z.; Zhao, X.-L.; Wang, T.-G. *J. Solid State Chem.* **2003**, *32*, 32, and references cited therein.
- (4) (a) Fujita, M.; Nagao, S.; Ogura, K. *J. Am. Chem. Soc.* **1995**, *117*, 1649. (b) Abrahams, B. F.; Batten, S. R.; Grannas, M. J.; Hamit, H.; Hoskins, B. F.; Robson, R. *Angew. Chem., Int. Ed.* **1999**, *38*, 1475. (c) Hong, M. C.; Zhao, Y. J.; Su, W. P.; Cao, R.; Fujita, M.; Zhou, Z. Y.; Chan, A. S. C. *Angew. Chem., Int. Ed.* **2000**, *39*, 2468. (d) Su, C. Y.; Cai, Y. P.; Chen, C. L.; Lissner, F.; Kang, B. S.; Kaim, W. *Angew. Chem., Int. Ed.* **2002**, *41*, 3371. (e) Costes, J.-P.; Dahan, F.; Nicodeme, F. *Inorg. Chem.* **2003**, *42*, 6556. (f) Wan, S. Y.; Li, Y. Z.; Okamura, T.; Fan, J.; Sun, W. Y.; Ueyama, N. *Eur. J. Inorg. Chem.* **2003**, 3183. (g) Su, C. Y.; Cai, Y. P.; Chen, C. L.; Smith, M. D.; Kaim, W.; zur Loye, H. C. *J. Am. Chem. Soc.* **2003**, *125*, 8595. (h) Zhao, W.; Song, Y.; Okamura, T. A.; Fan, J.; Sun, W. Y.; Ueyama, N. *Inorg. Chem.* **2005**, *44*, 3330.
- (5) Rao, C. N. R.; Natarajan, S.; Vaidhyanathan, R. *Angew. Chem., Int. Ed.* **2004**, *43*, 1466.
- (6) (a) Ruiz-Pérez, C.; Hernández-Molina, M.; Lorenzo-Luis, P.; Lloret, F.; Cano, J.; Julve, M. *Inorg. Chem.* **2000**, *39*, 3845. (b) Rodríguez-Martín, Y.; Hernández-Molina, M.; Delgado, F. S.; Pasán, J.; Ruiz-Pérez, C.; Sanchiz, J.; Lloret, F.; Julve, M. *CrystEngComm* **2002**, *4*, 522. (c) Delgado, F. S.; Sanchiz, J.; Ruiz-Pérez, C.; Lloret, F.; Julve, M. *CrystEngComm* **2004**, *6*, 443. (d) Delgado, F. S.; Ruiz-Pérez, C.; Sanchiz, J.; Lloret, F.; Julve, M. *CrystEngComm* **2006**, *8*, 507. (e) Delgado, F. S.; Ruiz-Pérez, C.; Sanchiz, J.; Lloret, F.; Julve, M. *CrystEngComm* **2006**, *8*, 530. (f) Pasán, J.; Sanchiz, J.; Ruiz-Pérez, C.; Campo, J.; Lloret, F.; Julve, M. *Chem. Commun.* **2006**, 2857. (g) Pasán, J.; Sanchiz, J.; Lloret, F.; Julve, M.; Ruiz-Pérez, C. *CrystEngComm* **2007**, *9*, 478.
- (7) (a) Mori, W.; Takamizawa, S. *J. Solid State Chem.* **2000**, *152*, 120. (b) Lo, S. M.-F.; Chui, S. S. Y.; Shek, L.-Y.; Lin, Z.; Zhang, X. X.; Wen, G.-H.; Williams, I. D. *J. Am. Chem. Soc.* **2000**, *122*, 6293. (c) Eddaoudi, M.; Kim, J.; Wachter, J. B.; Chae, H. K.; O'Keeffe, M.; Yaghi, O. M. *J. Am. Chem. Soc.* **2001**, *123*, 4368. (d) Chae, H. K.; Sierber-Perez, D. Y.; Kim, J.; Go, Y. B.; Eddaoudi, M.; Matzger, A. J.; O'Keeffe, M.; Yaghi, O. M. *Nature* **2004**, *427*, 523.
- (8) (a) Barthelet, K.; Riou, D.; Nogues, M.; Ferey, G. *Inorg. Chem.* **2003**, *42*, 1739. (b) Kumagai, H.; Chapman, K. W.; Kepert, C. J.; Kurmoo, M. *Polyhedron* **2003**, *22*, 1921. (c) Yang, S.-Y.; Long, L.-S.; Huang, R.-B.; Zheng, L.-S.; Ng, S. W. *Acta Crystallogr., Sect. E: Struct. Rep. Online* **2003**, *59*, m921. (d) Sanselme, M.; Greneche, J.-M.; Riou-Cavellec, M.; Ferey, G. *Solid State Sci.* **2004**, *6*, 853. (e) Fu, Y.-L.; Ren, J.-L.; Ng, S. W. *Acta Crystallogr., Sect. E: Struct. Rep. Online* **2004**, *60*, m1400.
- (9) (a) Ruiz-Pérez, C.; Lorenzo-Luis, P. A.; Hernández-Molina, M.; Laz, M. M.; Gili, P.; Julve, M. *Cryst. Growth Des.* **2004**, *4*, 57. (b) Fabelo, O.; Cañadillas-Delgado, L.; Delgado, F. S.; Lorenzo-Luis, P.; Laz, M. M.; Julve, M.; Ruiz-Pérez, C. *Cryst. Growth Des.* **2005**, *5*, 1163. (c) Fabelo, O.; Cañadillas-Delgado, L.; Pasán, J.; Ruiz-Pérez, C.; Julve, M. *CrystEngComm* **2006**, *8*, 338. (d) Cañadillas-Delgado, L.; Fabelo, O.; Ruiz-Pérez, C.; Delgado, F. S.; Julve, M.; Hernández-Molina, M.; Laz, M.; Lorenzo-Luis, P. *Cryst. Growth Des.* **2006**, *6*, 87. (e) Fabelo, O.; Pasán, J.; Lloret, F.; Julve, M.; Ruiz-Pérez, C. *CrystEngComm* **2007**, *9*, 815. (f) Fabelo, O.; Pasán, J.; Lloret, F.; Julve, M.; Ruiz-Pérez, C. *Inorg. Chem.* **2008**, *47*, 3568. (g) Ruiz-Pérez, C.; Fabelo, O.; Pasán, J.; Cañadillas-Delgado, L.; Delgado, F. S.; Labrador, A.; Lloret, F.; Julve, M. *Cryst. Growth Des.* **2008**, in press.
- (10) Duisenberg, A. J. M. (DIRAX). *J. Appl. Crystallogr.* **1992**, *25*, 92.
- (11) Sheldrick, G. M. *SHELX97, Programs for Crystal Structure Analysis*, release 97-2; Institut für Anorganische Chemie der Universität: Göttingen, Germany, 1998.

Table 1. Crystal Data and Details of the Structure Determination for the Complexes **1** and **2**

compound	1	2
formula	C ₅ H ₇ CoO ₇	C ₅ H ₇ CoO ₇
<i>M</i>	238.04	238.04
cryst syst	triclinic	monoclinic
space group	<i>P</i> 1	<i>P</i> 2 ₁ / <i>n</i>
<i>a</i> , Å	6.9104(7)	9.4860(4)
<i>b</i> , Å	7.4253(9)	6.0463(3)
<i>c</i> , Å	8.2544(6)	14.1134(5)
α, deg	90.397(8)	
β, deg	109.835(7)	104.901(4)
γ, deg	93.137(8)	
<i>V</i> , Å ³	397.68(7)	782.26(6)
<i>Z</i>	2	4
index ranges	−7 ≤ <i>h</i> ≤ 7 −8 ≤ <i>k</i> ≤ 8 −9 ≤ <i>l</i> ≤ 9	−12 ≤ <i>h</i> ≤ 10 −7 ≤ <i>k</i> ≤ 7 −17 ≤ <i>l</i> ≤ 18
<i>T</i> , K	293(2)	100(2)
ρ _{calc} , Mg m ^{−3}	1.988	2.021
λ(Mo Kα), Å	0.710 73	0.710 73
μ(Mo Kα), mm ^{−1}	2.162	2.198
R1, <i>I</i> > 2σ(<i>I</i>) (all)	0.0224 (0.0241)	0.0289 (0.0442)
wR2, <i>I</i> > 2σ(<i>I</i>) (all)	0.0594 (0.0600)	0.0638 (0.0699)
measd reflns	2766	4365
indep reflns (<i>R</i> _{int})	1112 (0.014)	1740 (0.025)
cryst size	0.20 × 0.15 × 0.15	0.20 × 0.14 × 0.10

Table 2. Selected Bond Lengths (Å), Angles (deg), and Intermolecular Contacts in **1**^a

Bond Lengths			
Co1–O1	2.055(2)	Co2–O2 ^{d-1}	2.078(2)
Co1–O3	2.037(2)	Co2–O4	2.092(2)
Co1–O1w	2.152(3)	Co2–O2w	2.100(2)
Bond Angles			
O1–Co1–O1w	85.29(8)	O4–Co2–O2 ^{d-1}	91.18(7)
O1–Co1–O3	90.35(8)	O2w–Co2–O2 ^{d-1}	86.43(9)
O1w–Co1–O3	85.72(8)	O2w–Co2–O4	96.09(8)
Intermolecular O···O Distances			
O2···O3w ^{a-1}	2.973(6)	O3w···O3w ^{c-1}	2.174(11)
O2···O4w ^{a-1}	3.024(4)	O3w···O4w ^{c-1}	2.783(9)
O1w···O4w ^{b-1}	2.856(5)	O3w···O4w	1.934(9)
O1w···O4w ^{c-1}	2.953(6)		

^a Symmetry code: a-1 = *x* + 1, *y* + 1, *z* + 1; b-1 = *x*, *y* + 1, *z*; c-1 = −*x*, −*y*, −*z* − 1, d-1 = 1 − *x*, 1 − *y*, −*z*.

carried out with *PARST97*,¹² *PLATON*,¹³ and *DIAMOND*¹⁴ programs. Selected bond lengths and angles together with hydrogen bonds are listed in Tables 2 (**1**) and 3 (**2**).

Crystallographic data (excluding structure factors) for the structures **1** and **2** have been deposited at the Cambridge Crystallographic Data Centre with CCDC reference numbers XXXX and XXXX, respectively.

Physical Techniques. Magnetic susceptibility measurements on polycrystalline samples of **1** and **2** were carried out on a Quantum Design SQUID magnetometer in the temperature range 1.9–300 K operating at 1 T (*T* ≥ 50 K) and 250 G (*T* > 50 K). Diamagnetic corrections of the constituent atoms for **1** and **2** were estimated from Pascal's constants¹⁵ as −201 × 10^{−6} cm³ mol^{−1} (per two Co^{II} ions). Corrections for the magnetization of the sample holder were also performed.

Results and Discussion

Description of the Structures. Compound 1. The structure of **1** consists of a three-dimensional MOF network

Table 3. Selected Bond Lengths (Å), Angles (deg), and Hydrogen Bonds in **2**^a

Bond Lengths			
Co1–O2 ^{e-2}	2.105(2)	Co2–O4	2.032(2)
Co1–O3	2.043(2)	Co2–O1w	2.1161(15)
Co1–O1w	2.1520(14)	Co2–O2w	2.116(2)
Bond Angles			
O3–Co1–O2 ^{e-2}	89.60(7)	O4–Co2–O1w	92.34(6)
O3–Co1–O1w	92.01(6)	O1w–Co2–O2w	89.45(7)
O1w–Co1–O2 ^{e-2}	88.38(6)	O2w–Co2–O4	90.92(7)
Hydrogen Bonds			
D–H···A	<i>d</i> (D···A) (Å)	<i>d</i> (H···A) (Å)	∠(D–H···A) (deg)
O1w–H1wA···O1 ^{a-2}	2.549(3)	1.73(4)	165(4)
O1w–H1wB···O3w ^{b-2}	2.656(3)	1.82(6)	168(3)
O2w–H2wB···O3w ^{b-2}	2.859(3)	2.03(7)	152(6)
O2w–H2wA···O2 ^{c-2}	2.655(2)	1.84(3)	169(4)
O3w–H3wB···O1 ^{d-2}	2.657(2)	1.80(2)	173(3)
O3w–H3wA···O3w ^{d-2}	2.804(3)	2.01(8)	138(6)

^a Symmetry code: a-2 = −*x* + 1/2 + 1, *y* − 1, −*z* + 1/2; b-2 = *x* + 1, *y*, *z*; c-2 = −*x* + 2, −*y* + 2, −*z* + 1; d-2 = −*x* + 1/2, *y*, −*z* + 1/2, e-2 = *x*, −1 + *y*, *z*.

with open channels where crystallization water molecules are embedded. The MOF is based on (4,4) rectangular layers of *trans*-[Co₂(H₂O)₂]²⁺ cations extending in the *bc* plane where the fully deprotonated bta⁴⁻ anion and acts as a 4-fold connector and the *trans*-diaquacobalt(II) cations act as 4-fold nodes (Figure 1a). The values of the intralayer Co···Co separation corresponding to the edges of the rectangles are 7.4253(9) Å (Co2···Co2^{e-1}; e-1 = *x*, 1 + *y*, *z*) and 8.2544(6) Å (Co2···Co2^{f-1}; f-1 = *x*, *y*, 1 + *z*). These layers are stacked along the *a* axis, and they are connected through *trans*-[Co₁(H₂O)₂]²⁺ units to form a three-dimensional [8⁴] network (Figure 1b). The crystallization water molecules are anchored in the pores and they are interconnected along the *b* axis (Figure 2a) through extensive hydrogen bonds involving some of the carboxylate O atoms and the coordinated water molecules (see the third section of Table 2). These pores exhibit a somewhat distorted rectangular shape of dimensions ca. 8.0 × 6.0 Å and a hydrophilic character because the coordination water molecules of the diaquacobalt(II) fragments are pointing toward the inner portion of the cavity (Figure 2b). Remarkably, two faces of the channel are formed by bta ligands with the benzene ring exposed to the cavity. The potential solvent-accessible void volume space in **1** is 74.1 Å³, a value that represents 18.6% of the volume of the unit cell.

The crystal structure of **1** can be alternatively described as corrugated (4,4) rectangular layers of *anti-syn* carboxylate-bridged Co^{II} ions extended in the *ab* plane, which are linked through bta ligands to build the three-dimensional structure (Figure 3). The values of the Co···Co separation through the single carboxylate bridge are 4.9313(5) (Co1···Co2^{b-1}; b-1 = *x*, *y* + 1, *z*) and 5.2083(5) Å (Co1···Co2), both being the shortest metal–metal distances in the three-dimensional network.

Two crystallographically independent Co atoms (Co1 and Co2) occur in **1**, both lying on crystallographic inversion sites (Figure 4). They are six-coordinated in octahedral environments, being slightly elongated at Co1 and quasi-

(12) Nardelli, M. J. *Appl. Crystallogr.* **1995**, *28*, 659.

(13) Spek, A. L. *J. Appl. Crystallogr.* **2003**, *36*, 7.

(14) *DIAMOND 2.1d*; Crystal Impact GbR: Bonn, Germany, 2000.

(15) Earnshaw, A. *Introduction to Magnetochemistry*; Academic Press: London, 1968.

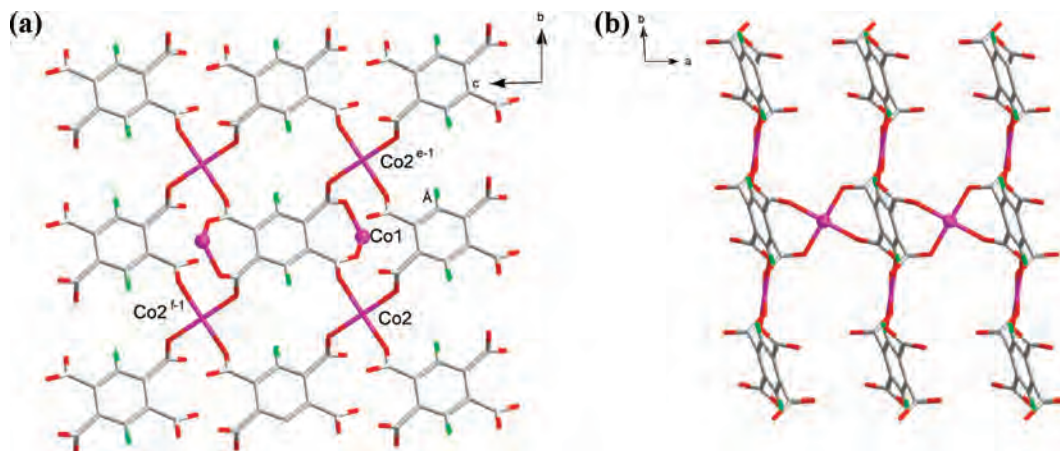


Figure 1. (a) Projection along the a axis of the (4,4) rectangular grid formed through $[\text{Co}_2(\text{bta})_2]^{2-}$ units including two Co1 atoms (pink spheres) to illustrate the 6-fold connector role of the bta^{4-} ligand. The coordinated and free water molecules have been omitted for the sake of clarity. (b) Perspective view along the c axis of the interconnection of the previous (4,4) rectangular layers through the Co1 atoms (drawn as pink spheres), with the water molecules being skipped for clarity.

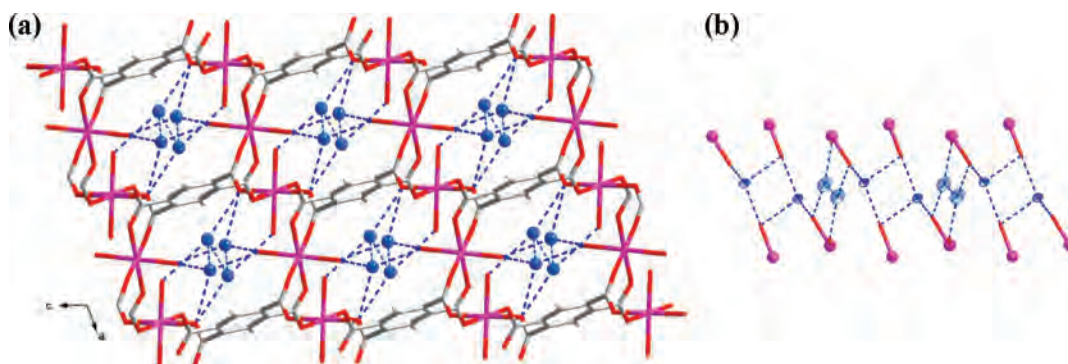


Figure 2. (a) Projection along the b axis of the three-dimensional crystal structure of **1** showing the crystallization water molecules anchored in the pores. (b) View of the water arrangement within the pores in **1**. The hydrogen bonds are drawn as blue dashed lines.

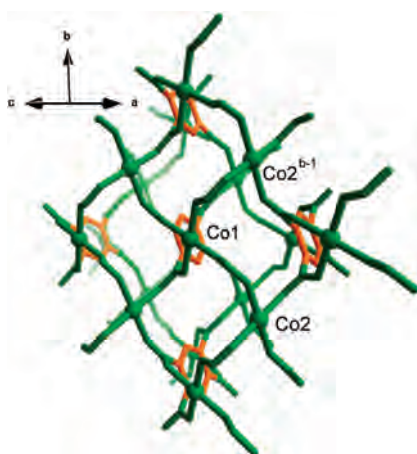


Figure 3. Projection along the [101] direction of the three-dimensional structure of **1**, showing the rectangular layer of *anti-syn* carboxylate-bridged Co atoms (green color). The benzene rings of the bta^{4-} ligand (orange color) show their bridging role between adjacent rectangular cobalt layers.

ideal at Co2, with geometric values ϕ and s/h of 58.19° and 1.25 (Co1) and 59.57° and 1.22 (Co2) ($\phi = 60^\circ$ and $s/h = 1.22$ for an ideal octahedral environment).¹⁶ The equatorial planes around the Co atoms are built up by four carboxylate O atoms, O1, O3, O1^{g-1}, and O3^{g-1} (Co1) and O2^{d-1}, O2^{h-1}, O4, and O4ⁱ⁻¹ (Co2) [symmetry code: $g-1 = x, 1-y, -z$;

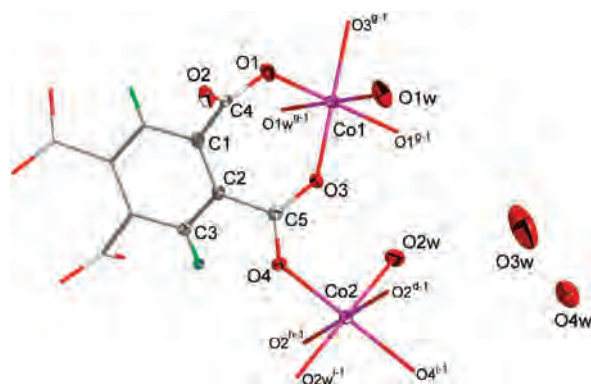


Figure 4. Perspective view of a fragment of the structure of **1** showing the two crystallographically independent Co atoms together with the atom numbering scheme. Thermal ellipsoids (drawn at the 50% probability level) have been used to denote the crystallographically independent unit.

$d-1 = 1-x, 1-y, -z$; $h-1 = x, -1+y, z$; $i-1 = 1-x, -y, -z$], while the apical positions are filled by two coordination water molecules, O1w^{g-1} and O1w^{e-1} (Co1) and O2w and O2wⁱ⁻¹ (Co2). The mean values of the equatorial Co–O_{carboxylate} bond distances are 2.044(3) and 2.084(3) Å for Co1 and Co2, respectively, and they are somewhat shorter than the axial Co–O_w bond lengths 2.156(4) (Co1) and 2.099(3) (Co2) Å. These values are in agreement with those previously reported for other bta-containing cobalt(II) complexes.^{9c} The bta^{4-} group in **1** is

(16) Stiefel, E. I.; Brown, G. F. *Inorg. Chem.* **1972**, *11*, 434.

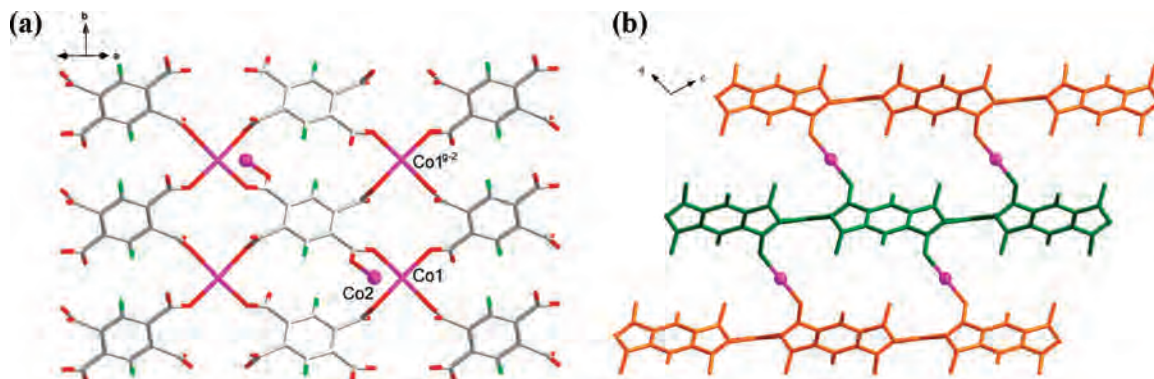


Figure 5. (a) Projection toward the (101) plane of the (4,4) rectangular grid in **2** constituted by the Co1bta⁴⁻ units with the inclusion of two Co2 atoms (pink spheres) to illustrate the 6-fold connector role of the bta⁴⁻ ligand. (b) View along the *b* axis showing the interconnection of the previous (4,4) rectangular layers through the Co2 atoms (pink spheres). Water molecules have been skipped for the sake of clarity.

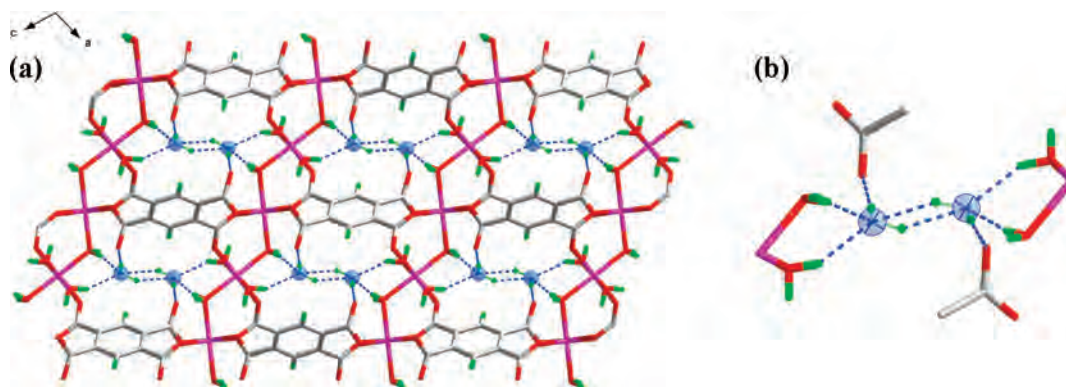


Figure 6. (a) Projection along the *b* axis of the three-dimensional crystal structure of **2** showing the crystallization water molecules anchored in the pores. (b) View of the water arrangement within the pores in **2**. The hydrogen bonds are drawn as blue dashed lines.

a six-fold connector, which connects four in-plane Co2 atoms to form the (4,4) rectangular network and two out-of-plane Co1 atoms to link the layers [$\text{Co1} \cdots \text{Co1}^{j-1}$; $j-1 = 1 + x$, y , $1 + z = 8.7852(9) \text{ \AA}$]. The bta⁴⁻ ligand lies across the inversion center located in the middle of the aromatic ring. It adopts simultaneously bis-bidentate (through O1 and O3 toward Co1 and their symmetry-related O atoms at Co1^{j-1}) and tetrakis-monodentate [through O2 and O4 toward Co2^{b-1} and Co2 and their symmetry-related O atoms toward Co2^{k-1} ($k-1 = x$, $1 + y$, $1 + z$) and Co2ⁱ⁻¹] coordination modes. The values of the dihedral angle between the plane defined by the benzene ring and those of the carboxylate groups are 39.58(14) and 73.59(13)°.

Compound 2. The crystal structure of **2** consists of an open three-dimensional MOF, with crystallization water molecules being hosted in the channels. As in **1**, the structure of **2** is based on (4,4) rectangular layers of *trans*-[Co1(H₂O)₂]²⁺ units connected through tetradeprotonated bta⁴⁻ anions, which extend in the (101) plane; the bta⁴⁻ groups and the *trans*-diaquacobalt(II) units within each layer acts as four-fold connectors (Figure 5a). These layers are linked through [Co2(H₂O)₄]²⁺ cations along the [101] direction, leading to a three-dimensional network (Figure 5b). The structure exhibits hydrophilic channels along the *b* axis of dimensions ca. $4.0 \times 5.0 \text{ \AA}^2$, where the O3w and O3w^{d-2} [symmetry code: $d-2 = 0.5 - x$, y , $0.5 - z$] crystallization water molecules are hosted (Figure 6a). These molecules build up dimeric water motifs that are anchored to the host

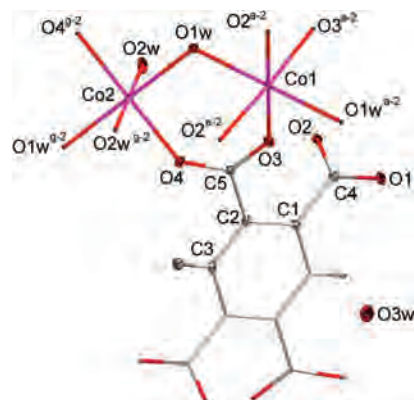


Figure 7. Perspective view of a fragment of the structure of **2** showing the two crystallographically independent Co atoms together with the atom numbering scheme. Thermal ellipsoids (drawn at the 50% probability level) have been used to denote the crystallographically independent unit.

matrix through hydrogen bonds involving coordinated water molecules and uncoordinated carboxylate O atoms (Figure 6b and the bottom of Table 3). The potential solvent-accessible void volume space in **2** is 96.5 \AA^3 , that is, ca. 12.3% per unit cell.

Two crystallographically independent Co atoms (Co1 and Co2) occur in **2**. Co1 is located on a two-fold rotation axis, whereas Co2 is placed on an inversion center (Figure 7). Both metal atoms are six-coordinated in slightly elongated (Co1) and somewhat compressed (Co2) octahedral environments, with geometric values ϕ and s/h of 58.10° and 1.24 (Co1) and 61.38° and 1.20 (Co2).¹⁶ The equatorial plane of

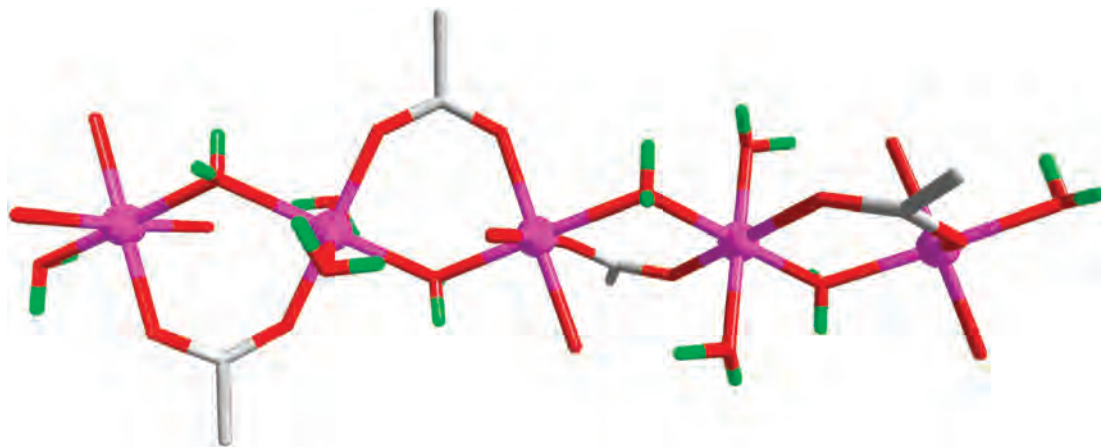


Figure 8. Perspective view of a fragment of the structure of **2** showing the regular alternating of Co1 and Co2 atoms through the aqua and *syn-syn* carboxylate bridges.

Co1 is built up by the O3, O2^{e-2}, O3^{a-2}, and O2^{a-2} carboxylate O atoms ($e-2 = x, -1 + y, z; a-2 = 1.5 - x, -1 + y, 0.5 - z$), while the apical positions are filled by the two O1w and O1w^{a-2} coordination water molecules. The equatorial plane at Co2 is formed by four coordination water molecules (O1w and O2w and their symmetry-related ones), whereas the axial positions are filled by two carboxylate O atoms (O4 and O4^{s-2}; $g-2 = 2 - x, 1 - y, 1 - z$). The mean values of the equatorial Co–O bond distances are 2.100(2) (at Co1) and 2.116(3) (at Co2) Å, and they are somewhat shorter (Co1)/longer (Co2) than the axial bond lengths, 2.1520(14) Å (Co1) and 2.032(2) Å (Co2) for the elongated/compressed octahedral environments. The two crystallographically independent Co atoms regularly alternate along the [101] direction, being bridged by a water molecule and a *syn-syn* carboxylate group (Figure 8). The values of the angle at the aqua bridge and the Co1⋯Co2 distance are 120.78(7)° and 3.7108(2) Å, respectively. This last value is much smaller than the shortest interchain metal–metal separation through the bta⁴⁻ skeleton [6.0463(7) Å]. The bta⁴⁻ ligand in **2** straddles the center of symmetry, and it adopts a hexakis-monodentate coordination mode through O3, O2, and O4 toward Co1, Co1^{h-2}, and Co2, respectively, and the same atoms through the inversion center ($h-2 = x, 1 + y, z$). The average value for the C–O bond distances in the carboxylate groups is 1.269(2) Å, in agreement with compound **1**. The values of the dihedral angles between the plane defined by the benzene ring and those of the carboxylate groups are 28.89(8)° and 69.22(7) Å. These values are rather close to those observed in **1**.

Magnetic Properties of 1 and 2. Compound 1. The thermal dependence of the $\chi_M T$ product (with χ_M being the magnetic susceptibility per Co^{II} ion) is shown in Figure 9. At room temperature, $\chi_M T$ is equal to 2.75 cm³ mol⁻¹ K (μ_{eff} per Co^{II} = 4.69 μ_B), a value that is greater than expected for a high-spin Co^{II} ion through the spin-only formula, ca. 1.87 cm³ mol⁻¹ K with $g = 2.0$ ($\mu_{\text{eff}} = 3.87 \mu_B$). This is due to the occurrence in **1** of an unquenched orbital contribution typical of the ⁴T_{1g} ground state in octahedral cobalt(II)

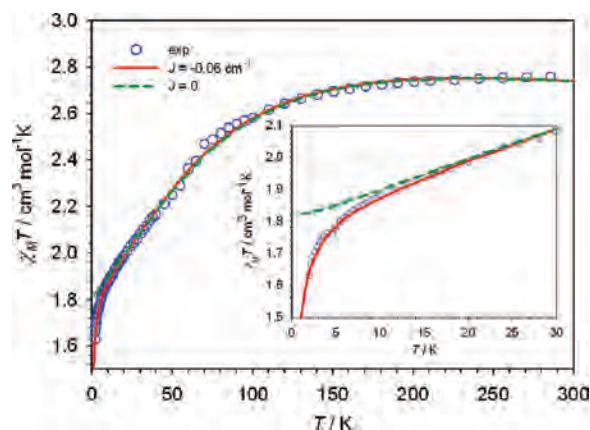


Figure 9. $\chi_M T$ vs T plot of **1**: (○) experimental data; (--- and —) best-fit curves through the Hamiltonian of eq 1 with $J = 0$ and $J = 0.06 \text{ cm}^{-1}$, respectively (see text). The inset shows a detail of the low-temperature region.

complexes.¹⁷ Upon cooling, $\chi_M T$ continuously decreases, reaching a value of 1.63 cm³ mol⁻¹ K at 1.9 K. This value is close or slightly below the expected one for a magnetically isolated Co^{II} ion ($\chi_M T \approx 1.75 \text{ cm}^3 \text{ mol}^{-1} \text{ K}$),¹⁸ indicating the occurrence, if any, of a very weak antiferromagnetic interaction. No maximum of the magnetic susceptibility is observed in the χ_M versus T plot. So, the decrease of $\chi_M T$ at high temperature is due to the depopulation of the higher energy Kramers doublets of the Co^{II} centers.

In fact, we can reproduce the magnetic behavior of **1** from room temperature until 20 K through the Hamiltonian of eq 1, which considers all of the Co^{II} ions to be magnetically isolated.

$$\hat{H} = \alpha\lambda\hat{L}\hat{S} + \Delta\left(\hat{L}_z^2 - \frac{2}{3}\right) + \beta H(-\alpha\hat{L} + g_e\hat{S}) \quad (1)$$

The first term of this Hamiltonian accounts for the spin–orbit coupling effects, where λ is the spin–orbit coupling constant and α is defined as $\alpha = A\kappa$, with A being a parameter whose

(17) Kahn, O. *Molecular Magnetism*; VCH Publishers: New York, 1993.

(18) (a) Dominguez, S.; Mederos, A.; Gili, P.; Rancel, A.; Rivero, A. E.; Brito, F.; Lloret, F.; Solans, X.; Ruiz-Pérez, C.; Rodríguez, M. L.; Brito, I. *Inorg. Chim. Acta* **1997**, 255, 367. (b) Rodríguez, A.; Sakiyama, H.; Masciocchi, N.; Galli, S.; Gálvez, N.; Lloret, F.; Colacio, E. *Inorg. Chem.* **2005**, 44, 8399.

value depends on the strength of the crystal field [its value varies between $3/2$ (weak crystal field) and 1 (strong crystal field)]¹⁹ and κ being the orbital reduction factor. The inclusion of the A factor is due to the use of the T–P isomorphism.²⁰ That is, A appears to distinguish between the matrix elements of the orbital angular momentum operator calculated with the wave functions of the $4T_{1g}$ ground-state term and those calculated with the use of the P basis ($11, 1$), $11, 0$), and $11, -1$). So, A can be defined by the symbolic equation $\mathbf{L}(T_{1g}) = -A\mathbf{L}(P)$. The second factor of this Hamiltonian is the one-center operator responsible for the axial distortion of the six-coordinated Co^{II} ion, with Δ being the energy gap between the singlet $4A_2$ and doublet $4E$ levels issued from the splitting of the orbital triplet $4T_{1g}$ ground state under an axial distortion. The last term is the Zeeman interaction. Finally, the two crystallographically independent Co^{II} ions in **1** (CoO_6 chromophore for both metal atoms) were considered to be equivalent in order to avoid overparametrization. The best-fit parameters through this assumption by using matrix diagonalization techniques²¹ are as follows: $\alpha = 1.15(1)$, $\Delta = -749(10) \text{ cm}^{-1}$, and $\lambda = -150(5) \text{ cm}^{-1}$. The corresponding calculated curve (dashed line in Figure 9) reproduces well the magnetic data from room temperature to ca. 20 K. At lower temperatures, the magnetic data are clearly below the calculated ones, indicating the occurrence of a weak antiferromagnetic coupling.²²

Concerning the possibility of the occurrence of a magnetic interaction in **1**, two exchange pathways can be considered in **1**: the bridging bta through the aromatic ring with $\text{Co}\cdots\text{Co}$ separations larger than 7.4 Å and the carboxylate–bta bridge in the *anti*–*syn* coordination mode with a $\text{Co}\cdots\text{Co}$ distance of ca. 5.0 Å. Previous magnetostructural studies of bta-bridged cobalt(II) complexes have shown that the first exchange pathway is unable to mediate any significant magnetic coupling.^{9e} As far as the second pathway is concerned, recent magnetostructural studies have evidenced the poor ability of the *anti*–*syn* carboxylate bridge to mediate significant magnetic interactions between high-spin Co^{II} ions in most of the cases.²³ Moreover, this pathway can also yield

weak ferromagnetic interactions²⁴ because it was observed in the layered compound $[\text{Co}(\text{OOCCH}_2\text{OPh})_2(\text{H}_2\text{O})_2]_n$ ($\text{PhOCH}_2\text{COOH}$ = phenoxyacetic acid).²⁵ In the light of these previous observations, we can assume that the observed thermal dependence of $\chi_{\text{M}}T$ values for **1** in Figure 9 is mainly due to spin–orbit coupling and the effects of the antiferromagnetic coupling only appear at very low temperatures ($T < 20 \text{ K}$). In this low range of temperatures, the high-spin Co^{II} ions can be viewed as effective spin doublets ($S_{\text{eff}} = 1/2$) with a Landé factor g_0 (eq 2), which corresponds to the ground-state Kramers doublet. So, the $\chi_{\text{M}}T$ value for this ground-state doublet is given by eq 3.

$$g_0 = \frac{10 + 2\alpha}{3} \quad (2)$$

$$\chi_{\text{M}}T = \frac{N\beta^2}{3k} g_0^2 S(S+1) = \frac{N\beta^2}{4k} g_0^2 \quad (3)$$

In a recent report,²⁶ we have proposed an approach to analyzing the magnetic data of compounds with six-coordinated high-spin Co^{II} ions that is valid in the limit of the weak magnetic coupling as compared to the spin–orbit coupling, $|J/\lambda| < 0.1$. This approach allows the Co^{II} ion in axial symmetry to be treated as an effective spin doublet ($S_{\text{eff}} = 1/2$), which is related with the real spin ($S = 3/2$) by $S_{\text{eff}} = (3/5)S$. In this respect, to describe the magnetic exchange in **1**, we can use the expression for the magnetic susceptibility of a square layer of interacting spin doublets that was proposed by Lines (eq 4).^{23c,27} This equation is only valid when the ground-state spin doublet is the only populated level ($T < 30 \text{ K}$).

$$\chi_{\text{M}} = \frac{9N\beta^2}{25|J|} g_0^2 \left\{ 3\Theta + \sum_{n=1}^6 \frac{C_n}{\Theta^{n-1}} \right\}^{-1} \quad (4)$$

with $\Theta = 12kT/25|J|$, $C_1 = 4$, $C_2 = 2.667$, $C_3 = 1.185$, $C_4 = 0.149$, $C_5 = -0.191$, and $C_6 = 0.001$.

In order to take into account the magnetic susceptibility in the whole temperature range and following our approach, we replace the value of g_0 by the $G(T, J)$ function (eq 5)

$$G(T, J) = G(T) + \frac{n}{2} \Delta g P_0 \quad (5)$$

where $G(T)$ represents the magnetic behavior of a magnetically isolated Co^{II} ion, which can be calculated through eq 6 and which is derived from eq 3 (χ_{M} in this equation is computed by using the Hamiltonian of eq 1). $\Delta g P_0$ accounts for the variation of g_0 due to the magnetic interactions between the ground-state Kramers doublets (eqs 7 and 8), with n being the number of $\text{Co}\cdots\text{Co}$ interactions of each Co^{II} ion within the layer ($n = 4$ in the present case).

- (19) (a) Figgis, B. N.; Gerloch, M.; Lewis, J.; Mabbs, F. E.; Webb, G. A. *J. Chem. Soc. A* **1968**, 2086. (b) Gerloch, M.; Quedsted, P. N. *J. Chem. Soc. A* **1971**, 3729. (c) Herrera, J. M.; Bleuzen, A.; Dromzée, Y.; Julve, M.; Lloret, F.; Verdager, M. *Inorg. Chem.* **2003**, *42*, 7052. (d) Maspocho, D.; Domingo, N.; Ruiz-Molina, D.; Wurst, K.; Hernández, J. M.; Vaughan, G.; Rovira, C.; Lloret, F.; Tejada, J.; Veciana, J. *Inorg. Chem.* **2007**, *46*, 1627.
- (20) (a) Lines, M. E. *J. Chem. Phys.* **1971**, *55*, 2977. (b) De Munno, G.; Julve, M.; Lloret, F.; Faus, J.; Caneschi, A. *J. Chem. Soc., Dalton Trans.* **1994**, 1175. (c) De Munno, G.; Poerio, T.; Julve, M.; Lloret, F.; Viau, G. *New J. Chem.* **1998**, 299. (d) Sharma, A. K.; Lloret, F.; Mukherjee, R. *Inorg. Chem.* **2007**, *46*, 5128.
- (21) Cano, J. *VPMAG*, revision C03; Universities of Valencia and Barcelona: Valencia and Barcelona, Spain, 2004.
- (22) Maspocho, D.; Domingo, N.; Ruiz-Molina, D.; Wurst, K.; Hernández, J. M.; Vaughan, G.; Rovira, C.; Lloret, F.; Tejada, J.; Veciana, J. *Chem. Commun.* **2005**, 5035.
- (23) (a) Ruiz-Pérez, C.; Sanchiz, J.; Hernández-Molina, M.; Lloret, F.; Julve, M. *Inorg. Chim. Acta* **2000**, *298*, 202. (b) Ghoshal, D.; Mostafa, G.; Maji, T. K.; Zangrando, E.; Lu, T.-H.; Ribas, J.; Chaudhuri, N. R. *New J. Chem.* **2004**, *28*, 1204. (c) Delgado, F.-S.; Hernández-Molina, M.; Sanchiz, J.; Ruiz-Pérez, C.; Rodríguez-Martín, Y.; López, T.; Lloret, F.; Julve, M. *CrystEngComm* **2004**, *6*, 106.

- (24) (a) Delgado, F. S.; Sanchiz, J.; Ruiz-Pérez, C.; Lloret, F.; Julve, M. *Inorg. Chem.* **2003**, *42*, 5938. (b) Mishra, V.; Lloret, F.; Mukherjee, R. *Inorg. Chim. Acta* **2006**, *359*, 4053.
- (25) Rueff, J.-M.; Paulsen, C.; Souletie, J.; Drillon, M.; Rabu, P. *Solid State Sci.* **2005**, *7*, 431.
- (26) Lloret, F.; Julve, M.; Cano, J.; Ruiz, R.; Pardo, E. *Inorg. Chim. Acta* **2008**, in press. DOI: 10.1016/j.ica.2008.03.114.
- (27) (a) Lines, M. E. *J. Phys. Chem. Solids* **1970**, *31*, 1001.

$$[G(T)]^2 = \frac{4k}{N\beta^2} \chi_M T \quad (6)$$

$$\Delta g = -\frac{100J}{81\alpha\lambda}(\alpha + 2) \quad (7)$$

$$P_0 = \frac{\exp\left(-\frac{4\alpha\lambda}{kT}\right)}{3 + 2 \exp\left(-\frac{5\alpha\lambda}{2kT}\right) + \exp\left(-\frac{4\alpha\lambda}{kT}\right)} \quad (8)$$

The corresponding analysis of the magnetic data of **1** through eq 4 when g_0 is replaced by the $G(T, J)$ function leads to the following set of best-fit parameters: $J = -0.060(2) \text{ cm}^{-1}$, $\lambda = -149(10) \text{ cm}^{-1}$, $\alpha = 1.15(1)$, and $\Delta = -750(10) \text{ cm}^{-1}$. The theoretical curve (solid line in Figure 9) reproduces very well the magnetic data in the whole temperature range. The magnetic coupling in **1** is very weak, as expected, and the values of the λ , α , and Δ parameters lie within the range of those observed in other six-coordinated high-spin complexes.^{18–20}

Compound 2. The magnetic properties of **2** in the form of a $\chi_M T$ versus T plot (χ_M is the molar magnetic susceptibility for one Co^{II} ion) are shown in Figure 10. $\chi_M T$ at 300 K is $2.79 \text{ cm}^3 \text{ mol}^{-1} \text{ K}$ ($\mu_{\text{eff}} = 4.72 \mu_B$), a value that is as expected for a high-spin Co^{II} ion with an important orbital contribution. Upon cooling, $\chi_M T$ continuously decreases to reach a value of $0.25 \text{ cm}^3 \text{ mol}^{-1}$ at 1.9 K. A maximum of the magnetic susceptibility is observed in the χ_M versus T plot of **2** at 4.0 K. The occurrence of a maximum of χ_M at low temperature in **2** unambiguously reveals the presence of a significant antiferromagnetic interaction between the Co^{II} ions.

An inspection of the structure of **2**, and keeping in mind the very low efficiency of the extended bta bridge to mediate magnetic interactions evidenced by the previous magnetic analysis on **1**, led us to conclude that the magnetic properties of **2** have their origin in the μ -aqua/ μ -carboxylate cobalt(II) chains without any interchain magnetic coupling through the bta^{4-} ligand that connects them.

Following the above approach and from a magnetic point of view, complex **2** can be viewed as a uniform chain of antiferromagnetically interacting spin doublets. In this respect, the numerical expression derived by Bonner and

Fisher²⁸ (eq 9) can be used to analyze the magnetic susceptibility of **2**, where the g factor has been replaced by the $G(T, J)$ function with $n = 2$ (eqs 5–8).

$$\chi_M = \frac{N\beta^2}{kT} \times [G(T, J)]^2 \frac{0.25 + 0.074975x + 0.075235x^2}{1.0 + 0.9931x + 0.172135x^2 + 0.757825x^3} \quad (9)$$

with $x = (25/9) |J|/kT$.

The two crystallographically independent six-coordinated Co atoms that alternate regularly within the chain are considered equivalent in order to avoid the overparametrization in the fitting procedure. A very good fit (solid line in Figure 10) is obtained for the magnetic data of **2** in the whole temperature range through matrix diagonalization techniques with the following set of best-fit parameters: $J = -1.90 \text{ cm}^{-1}$, $\lambda = -144 \text{ cm}^{-1}$, $\alpha = 1.28$, and $\Delta = 460 \text{ cm}^{-1}$. The low value of the $|J/\lambda|$ quotient (0.013) justifies the use of the above approach.

A significant antiferromagnetic coupling between the Co^{II} ions through the double μ -aqua- μ -carboxylate bridge is obtained in **2** ($J = -1.90 \text{ cm}^{-1}$), with the carboxylate group exhibiting the *syn-syn* conformation. This value compares well with that recently reported for the analogous μ -aqua-bis(μ -carboxylate)dycobalt(II) core ($J = -1.2 \text{ cm}^{-1}$) in the complex of formula $[\text{Co}_2(\text{butca})(\text{H}_2\text{O})_5]_n \cdot 2n\text{H}_2\text{O}$ ($\text{H}_4\text{butca} = 1,2,3,4\text{-butanetetra-carboxylic acid}$),²⁹ where two carboxylate groups in the *syn-syn* conformation and a water molecule act as bridges between a pair of Co^{II} ions. The larger value of the angle at the bridging aqua ligand in **2** [$120.78(7)^\circ$] versus that in this last compound [$113.10(8)^\circ$] accounts for the somewhat greater antiferromagnetic coupling in **2**.

Conclusion

In the present study, two pyromellitate-containing cobalt(II) compounds of formula $[\text{Co}_2(\text{bta})(\text{H}_2\text{O})_4]_n \cdot 2n\text{H}_2\text{O}$ (**1** and **2**) were magnetostructurally characterized. The crystals were obtained by using the hydrothermal synthesis at two different temperatures, affording two different and stable three-dimensional networks. Their magnetic properties revealed the occurrence of very weak (**1**) and weak (**2**) antiferromagnetic interactions between the Co^{II} ions through carboxylate- bta^{4-} bridges with the *anti-syn* conformation (**1**) and across μ -aqua-bis(μ -carboxylate) (*syn-syn* conformation) (**2**). Our study shows how bta^{4-} can adopt different coordination modes in its complexes with the same metal ion, with the subtle structural changes associated with this situation having a relevant role in the observed magnetic behavior. The two coordination polymers obtained have small channels, with potential solvent-accessible void volume spaces of 18.6 (**1**) and 12.3% (**2**) per unit cell, values that are large enough to accommodate several crystallization

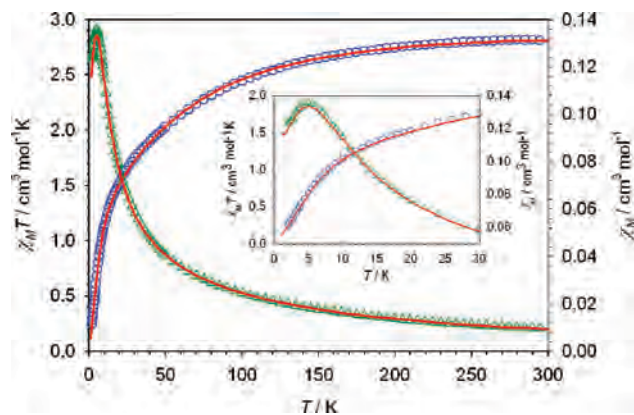


Figure 10. $\chi_M T$ (\circ) and χ_M (Δ) versus T plots of **2**. The solid lines are the best-fit curves through eq 9 (see text). The inset shows the region in the vicinity of the maximum of susceptibility.

- (28) (a) Bonner, J. C.; Fisher, M. E. *Phys. Rev. A* **1964**, *135*, 640. (b) Estes, W. E.; Gavel, D. P.; Hatfield, W. E.; Hodgson, D. *Inorg. Chem.* **1978**, *17*, 1415. (c) De Munno, G.; Poerio, T.; Julve, M.; Lloret, F.; Viau, G. *New J. Chem.* **1998**, 299.
- (29) Cañadillas-Delgado, L.; Fabelo, O.; Pasán, J.; Delgado, F. S.; Lloret, F.; Julve, M.; Ruiz-Pérez, C. *Inorg. Chem.* **2007**, *46*, 7458.

water molecules. The substitution of the guest water molecules that are trapped in these nets will be the subject of further studies.

Acknowledgment. Funding for this work is provided by the Ministerio Español de Educación y Ciencia through Projects MAT2004-03112, MAT2007-60660, CTQ2007-61690, and “Factoría de Cristalización” (Consolider-Ingenio2010, CSD2006-00015). F.S.D. and O.F. thank the Spanish Ministerio de Educación y Ciencia for post- and

predoctoral fellowships, respectively. L.C.-D. thanks the Gobierno Autónomo de Canarias for a predoctoral fellowship. Thanks are also extended to the Project CSD2006-00015 for a postdoctoral contract on behalf of J.P.

Supporting Information Available: X-ray crystallographic data in CIF format. This material is available free of charge via the Internet at <http://pubs.acs.org>.

IC800704Y